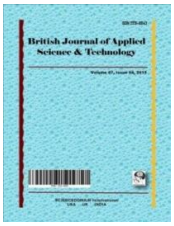

*British Journal of Applied Science & Technology*
*14(1): 1-14, 2016, Article no.BJAST.23177*
*ISSN: 2231-0843, NLM ID: 101664541*

**SCIENCEDOMAIN** *international*
www.sciencedomain.org

# Mechanical Properties of Healthy and *ex vivo* Onychomycosis Nails and the Influence of a Porphyrin-propylene Glycol Antifungal Formulation

**Amu Hosseinzoi[1], Federica Galli[2], Luca Incrocci[1] and Threes Smijs[1*]**

*[1]Department of Radiotherapy, Erasmus Medical Centre, Rotterdam, The Netherlands.*
*[2]Leiden Institute of Physics (LION), Leiden University, Leiden, The Netherlands.*

***Authors' contributions***

*This work was carried out in collaboration between all authors. Author TS designed the study, performed the statistical analysis, wrote the protocol and wrote part of the first draft of the manuscript. Additionally, she was responsible for the microbiological work at Erasmus MC and guidance of the AFM experiments at Leiden University. Author AH performed the AFM technical work and wrote important manuscript parts. Author FG guided the AFM experiments. Author LI critically reviewed the manuscript. All authors read and approved the final manuscript.*

***Article Information***

DOI: 10.9734/BJAST/2016/23177
Editor(s):
(1) Lesley Diack, School of Pharmacy and Life Sciences, Robert Gordon University, UK.
Reviewers:
(1) Farhana Tahseen Taj, K L E University, Karnataka, India.
(2) Somchai Amornyotin, Mahidol University, Bangkok, Thailand.
Complete Peer review History: http://sciencedomain.org/review-history/12827

***Original Research Article***

***Received 18th November 2015***
***Accepted 10th December 2015***
***Published 29th December 2015***

## ABSTRACT

**Aims:** To investigate nail penetration enhancing effectiveness of a novel drug formulation and ingredients, 40% propylene glycol (PG) and 40 μM multifunctional photosensitizer (MFPS). Proposed formulation was proven effective in photodynamic treatment (PDT) of *ex vivo* fungal infections of human nails (onychomycoses) and indirectly also to weaken nail's strength.
**Study Design:** To directly proof the effect of the novel formulation on nail's hardness Atomic Force Microscopy (AFM) was employed to measure small-distance forces. Based on indentations Young's moduli of healthy and *ex vivo* onychomycosis nails were calculated before and after treatment with the novel formulation. Changes in young's modulus can be related to changes in nail's strength and thus formulation effectiveness. Additionally, AFM imaging was employed to study topographical / roughness changes resulting from the treatments to both nail types. *Trichophyton mentagrophytes*, representative for clinical onychomycosis, was chosen to induce nail infections.

**Corresponding author: E-mail: g.smijs@erasmusmc.nl;*

**Place and Duration of Study:** AFM study was performed at Leiden Institute of Physics (Leiden University, The Netherlands). General study design, chemical and microbiological investigations took place at Erasmus MC (Rotterdam, The Netherlands).
**Methodology:** Tapping mode was used for imaging and contact mode for indentations. For each healthy and onychomycosis nail 5 to 6 spots of 8 x 8 µm on marked areas were studies (3-5 image scans and 5-10 indentations performed per spot). Young's moduli were calculated using the Hertz model.
**Results:** MFPS, PG and MFPS/PG affected healthy nail topography; roughness remained unchanged (PG; MFPS; MFPS/PG) or decreased (MFPS; MFPS/PG). Roughness of onychomycosis nails was lower compared to healthy nails and reduced after MFPS/PG treatment. Healthy nail Young's moduli varied (1-18 GPa) but decreased significantly after MFPS or PG treatment. Young's moduli of onychomycosis nails were lower compared to healthy nails and seemingly increased after MFPS/PG treatment.
**Conclusion:** Human nails are extremely inhomogeneous (strength / topography) thereby influencing topical drug response.

*Keywords: Onychomycosis; atomic force microscopy; nail; keratin; porphyrin; antifungal.*

## 1. INTRODUCTION

Onychomycosis is a common fungal infection that affects both finger- and toenails [1]. For reasons such as antifungal drug resistance and growing number of diabetic and cancer patients the incidence of this nail condition is still increasing [1,2]. Moreover, onychomycosis increases with age and since the population of elderly people is increasing this clinical condition may become a significant medical problem [3]. This fungal nail infection is mainly caused by dermatophytes, a group of fungi that colonises keratinised structures such as skin, hair and nails. Dermatophytic strains *Trichophyton rubrum* and *Trichophyton mentagrophytes* are most frequently isolated from nails from hands and feet. An important obstacle in particularly onychomycosis treatment is the localisation of the infection in and underneath the nail plate in combination with the hardness of the nail plate and thus low permeability to drugs. This nail's strength is the main reason for a frequent recurrence of the infection followed by long and thus expensive treatments. Moreover, common drugs mainly act on metabolic active fungal elements thereby leaving fungal conidia largely unaffected. This rigidity of nail is mediated by its keratin protein structure. The keratins of nails are arranged as numbers of coiled coils of α-helix-structured keratin proteins (see Fig. 1) of which the strength is determined by the number of -S-S- disulphide cross links in this structure mediated by sulphur-containing amino acids. In case of nail keratin, the number of SH-containing cysteine amino acid units is large [4] and apart from disulphide bridges within single keratin protein there is a large number of intermolecular disulphide bridges. Both factors cause the increased strength of nail compared to hair and skin keratin. Additionally, intra- and intermolecular hydrogen bonds result in strong, stable keratin fibres. Effective onychomycosis therapeutic formulations should therefore preferably increase the permeability of the nail plate and at the same time display antifungal effectiveness.

Our recent researches proved excellent *in vitro* and *ex vivo* antifungal effectiveness and nail penetration enhancement of a newly developed multifunctional porphyrin (see Fig. 2) for photodynamic treatment PDT [5,6]. This PDT requires light-activated agents, named photosensitisers, in combination with light of a proper wavelength and, depending on the reaction type, the presence of molecular oxygen. With our multifunctional photosensitiser (MFPS, 40 µM) formulated in 40% propylene glycol (PG) double PDT (28 J/cm$^2$ green light) within 48 hours resulted in 100% kill of *ex vivo* induced, extensive and invasive 35-day *T. mentagrophytes* onychomycosis [6]. Chemically induced nail penetration enhancing effects are mostly determined in drug penetration tests by measuring the amount of drug that penetrates the nail after chemical treatment. The aim of the present study is to directly proof contribution of our effective PDT formulation and individual components (40% PG, 40 µM MFPS) to increased permeability, and thus reduced stiffness, of healthy and *ex vivo* induced onychomycosis human nails. Additionally, we investigated the effect of this antifungal formulation and components to the nail's topography.

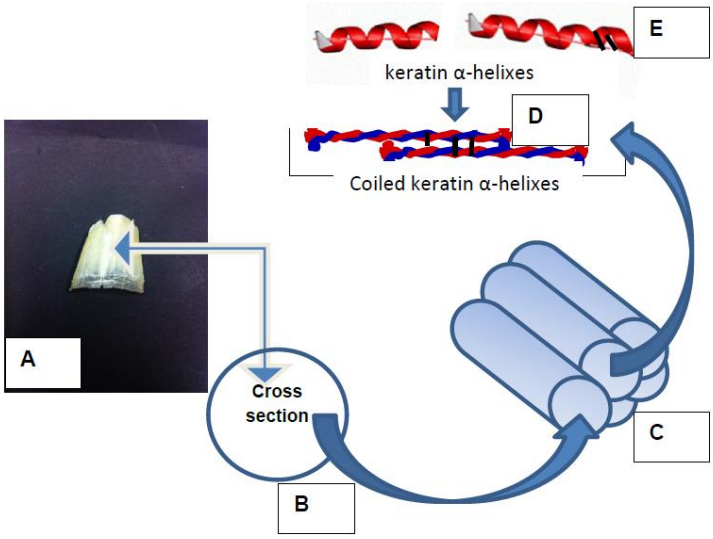


**Fig. 1. Schematic representation of nail keratin**

*A human nail plate (A) Shows in a cross-section (B) Numerous bundles (C) Each consisting of a number of coiled (D) α-helix keratin (E) Fibres. The strength of the nail's keratin is mainly caused by intramolecular α-helix protein S-S- bridges (E: black lines) and intermolecular disulphide links (black lines in D between a single helix and various coiled helixes)*

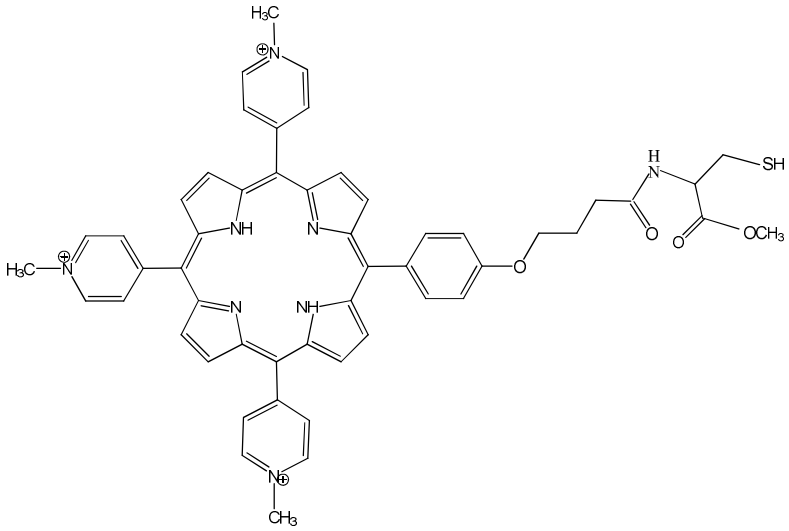


**Fig. 2. Structural formula of a novel multifunctional porphyrin developed for antifungal photodynamic treatment, 5,10,15-tris(4-N-methylpyridinium)-20-(4-(butyramido-methylcysteinyl)-hydroxyphenyl)-[21H,23H]-porphine trichloride**

We choose to use Atomic Force Microscopy (AFM). By scanning the surface of a material with a tens of nanometre's sharp probe attached at the end of an elastic beam (the cantilever), the AFM technique offers the possibility to image the sample's surface topography at high resolution (imaging) but also to measure small distance forces such as van der Waals forces, chemical bonding, electrostatic forces, magnetic forces etc. when the cantilever's tip is approaching the sample's surface. In contrast to scanning electron microscopy AFM does not require a vacuum nor does it require sample fixation. Both conditions are highly convenient when investigating chemical effects on material. Force measurements result from forces associated with interactions between cantilever tip and sample as function of the distance between these two

resulting in so-called force distance (F-D) curves or otherwise called force spectroscopy. Based on these F-D curves the Young's modulus for a certain material can be calculated. This modulus of elasticity is a mechanical property of an elastic material that measures the force that is needed to compress or stretch this material. Young's moduli values therefore represent the strength of a material like for instance our nail samples. The higher the Young's modulus the higher the stiffness of the material. For keratin-based biological material other than human nails Young's moduli have been determined to range from 1-4 GPa [7]. For bovine hoofs, the material that is often used to replace human nails in drug penetration studies, this value was measured 0.4 GPa [8]. This study applied AFM for both imaging and F-D measurements of healthy human nails before and after treatment with 40% PG, 40 µM MFPS or a combination of these two in our effective antifungal PDT formulation. In case of *ex vivo* induced onychomycosis nails F-D and imaging were both applied before and after treatment of the nails with the complete PDT formulation. Comparison of calculated Young's moduli may thus show the contribution of our antifungal formulation (and components) in changing the nails topography and/or its strength and therefore act as direct measure for the nail penetration enhancing efficiency of our MFPS drug on a sub-micron (nm) scale.

## 2. MATERIALS AND METHODS

### 2.1 Chemicals

MFPS (mol. wt: 987.5 g/mol; purity: 97%) was purchased from Buchem BV (Apeldoorn, The Netherlands).The MFPS stock solution (8 mM) was prepared in *Milli*-Q and stored at 4°C for no longer than 2 days. All other chemicals were purchased from Sigma-Aldrich Chemie (Zwijndrecht, The Netherlands). MFPS stock dilutions and 40% (v/v) PG solution were made in *Milli*-Q. The effective PDT formulation was prepared by diluting the MFPS stock solution in 40% PG (v/v in *Milli*-Q) to a final concentration of 40 µM.

### 2.2 Fungal Strain and Conidia Preparation

Clinical (onychomycosis) isolates of *T. mentagrophytes* were kindly provided by the Department of Medical Microbiology and Infectious Diseases from Erasmus Medical Centre (Rotterdam, the Netherlands) and cultured on Sabouraud dextrose agar (SDA, Sigma Aldrich Chemie GmbH, Schnelldorf, Germany) at room temperature (RT). Microconidia suspensions were prepared as described previously and stored in liquid nitrogen for no longer than 6 months [9,10]. Counting the number of colony forming units (cfu) on malt extract agar (MEA, Oxoid, Hampshire, UK) was used as a viability check.

### 2.3 Nails

#### 2.3.1 Healthy nails

Nail clippings (340-400 µm thick) were collected from the same middle finger of the same volunteer. Nails were cleaned with 70% ethanol for 3 minutes in an ultrasonic water bath, stored in sealed plastic bags (RT) and used within 2 months. To assure the same AFM starting point nails were, prior to any test treatment, alternately soaked in 70% isopropanol and sterile *Milli*-Q (twice) and dried to air (15 min).

#### 2.3.2 Onychomycosis nails

Middle finger healthy nails from the same nail donor as mentioned under 2.3.1, trimmed to 7-10 mg pieces, were disinfected by alternately soaking them twice in 70% isopropanol and sterile *Milli*-Q. Each nail was subsequently incubated in 100 µL*T. mentagrophytes* microconidia suspension (2.5-3 x $10^6$ cfu/mL), after 3 hours transferred to a 35-mm Petri dish positioned in a 96-mm Petri dish filled with 25 mL sterile *Milli*-Q and incubated at 37°C and 6.4% $CO_2$ for 14 days. At this time point the infection has penetrated the nail plate.[6] Additionally, onychomycosis nails were kindly provided by a volunteer suffering from a diagnosed *T. rubrum* nail infection.

### 2.4 AFM

#### 2.4.1 General information

All experiments were carried out with a Bruker Multimode 8 AFM equipped with Nanoscope 8.1 software (Bruker). The instrument was positioned on a table (acting as a vibration isolation system) inside a cabinet to reduce acoustic interference. Silicon cantilever probes with nominal 70 kHz (50-90 kHz) resonance frequency, 8 nm radius (18° half-cone angle) and average elastic constant of 1.8 N/m were used (AC240TS, Olympus corporation). The actual cantilever spring constant was determined experimentally for each measurement (5±1 N/m). All types of experiments were performed 2 to 3 times using different nail parts from the same nail clipping.

#### 2.4.2 Sample preparation

Both healthy and onychomycosis nails were (after indicated general pre-treatment) cut into small triangular pieces, firmly positioned on the AFM sample stub (the dorsal nail site on top), one of the corners of the nail triangle selected as study area and imaging and F-D measurements directly performed. After these untreated nail measurements, various test solutions (40 µM MFPS, 40% PG and / or 40 µM MFPS/40% PG) were applied to the nail on the AFM sample stub. The AFM sample stub was therefore transferred to a 35 mm Petri dish, the test solution applied topically such that the nail sample was just covered by the solution, the Petri dish closed and the nail subsequently incubated for 40 hours (RT). Superfluous test solution was then carefully removed with a tissue, the AFM sample stub positioned in the AFM instrument in exactly the same way as before the treatment and imaging and F-D again measured in the same area as before.

#### 2.4.3 Imaging

For each sample 5 to 6 spots of 8 x 8 µm were imaged (3-5 scans / spot) in tapping mode (ambient air). This mode is appropriate for most surfaces. Image resolution was set on 512x512 pixels and the scan rate on 2Hz (tip velocity 32 µm/s). Image roughness values were calculated using the following formula:

$$R_q = \sqrt{\frac{\sum z_i^2}{N}} \quad (1)$$

In equation (1) $Rq$ represents the root mean square rougness RMS (m), $z_i$ the height value (m) on a pixel and $N$ the number of total pixels.

#### 2.4.4 F-D measurements

F-D measurements were perfomed in contact mode on 3 to 5 spots in the same imaging area using 5 to 10 indentaions per spot (1Hz indentation rate). Young's modulus values were based on the average of young's moduli calculated from all indentations in all spots in the selected area.The Hertz model, describing the deformation behaviour of elastic materials [11], was used to fit F-D curves and calculate Young's modulus [12]:

$$F = \frac{4}{3}\frac{E}{1-\nu^2}\sqrt{r}\cdot\delta^{\frac{3}{2}} \quad (2)$$

In equation (2) $F$ represents the applied force (N), $r$ tip radius (m), $E$ theYoung's Modulus (Pa), $\nu$ the poisson ratio (also called the coefficient of expansion on the transverse axial, defined as the dimensionless negative ratio of transverse to axial strain) and $\delta$ the deformation at maximum load (m). This Hertz model (no adhesion) rather than the commonly applied Sneddon model was chosen because deformations in this study were not significantly larger than the tip radius. For all samples the assumed standard value of 0.3 [13] was used to calculate Young's moduli.

### 2.5 Statistical Analysis

Statistical data analysis was performed using Wilcoxon Signed-Ranks Test programmed in IBM SPSS statistics 21 with a critical level of significance of $p = 0.05$.

## 3. RESULTS AND DISCUSSION

### 3.1 MFPS, PG and MFPS/PG Formulation Affected Healthy Nail Topography

Fig. 3 shows the most representative images (left part) and corresponding profile lines (right) of the same fingernail clipping before and after a 40-hour treatment with 40 µM MFPS (Fig. 3A compared to Fig. 3B), 40% PG (Fig. 3C compared to Fig. 3D) and 40µM/40%PG (Fig. 3E compared to Fig. 3F). It may be noticed that all treatments resulted in topographical changes showing a more irregular surface with swellings (3D) and some holes in case of treatment with the complete PDT formulation (Fig. 3F). Differences between high (light) and low (dark) areas in the scanned sections didn't always increase after the treatments. When comparing images form Figs. 3A, 3C and 3E it may be noticed that different parts within one and the same nail clipping also show topographical differences. This may demonstrate the inhomogeneous character of the human nail plate, an observation that is confirmed by image roughness values calculated for selected spots (Table 1). Within selected healthy nail parts (prior to any treatment) both similar (resulting from spots from parts1 and 6) and different image roughness (resulting from spots from parts 2, 3, 4 and 5) could be detected. Based on the mean *Rq* values, covering all spots over the marked nail part area, only healthy untreated nail part 1 differed significantly in roughness form similar other parts. Because the a-numbered spots (selcted after treatment) may differ slightly from

similar numbered spots their *Rq* values cannot simply be compared and the mean $Rq$ was therefore again used for comparison.

Only in two occasions, following one of the MFPS and the MFPS/PG treatments, $Rq$ decreased (bold typed values in Table 1); generally, roughness didn't change.These observations differ partly from those given by Vaka et al. [14]. This group used AFM for topographical imaging studies of human nails before and after treatment with various nail penetration enhancing chemicals such as phosphoric acid, lactic acid and tartaric acid. For the higher, 10%, concentrations an increase rather than decrease in $Rq$ was found (exept for tartaric acid) while the lower tested, 1%, concentrations resulted in no change in $Rq$ when compared with untreated control nails. Differences in observations could be explained by novel chemical indentity and of our MFPS responsible for its efficient penetration enhancing efficacy. The nail penetration enhancing capacity of the MFPS was recently proven higher when compared to PG and other nail penetration enhacing chemicals [5,15].

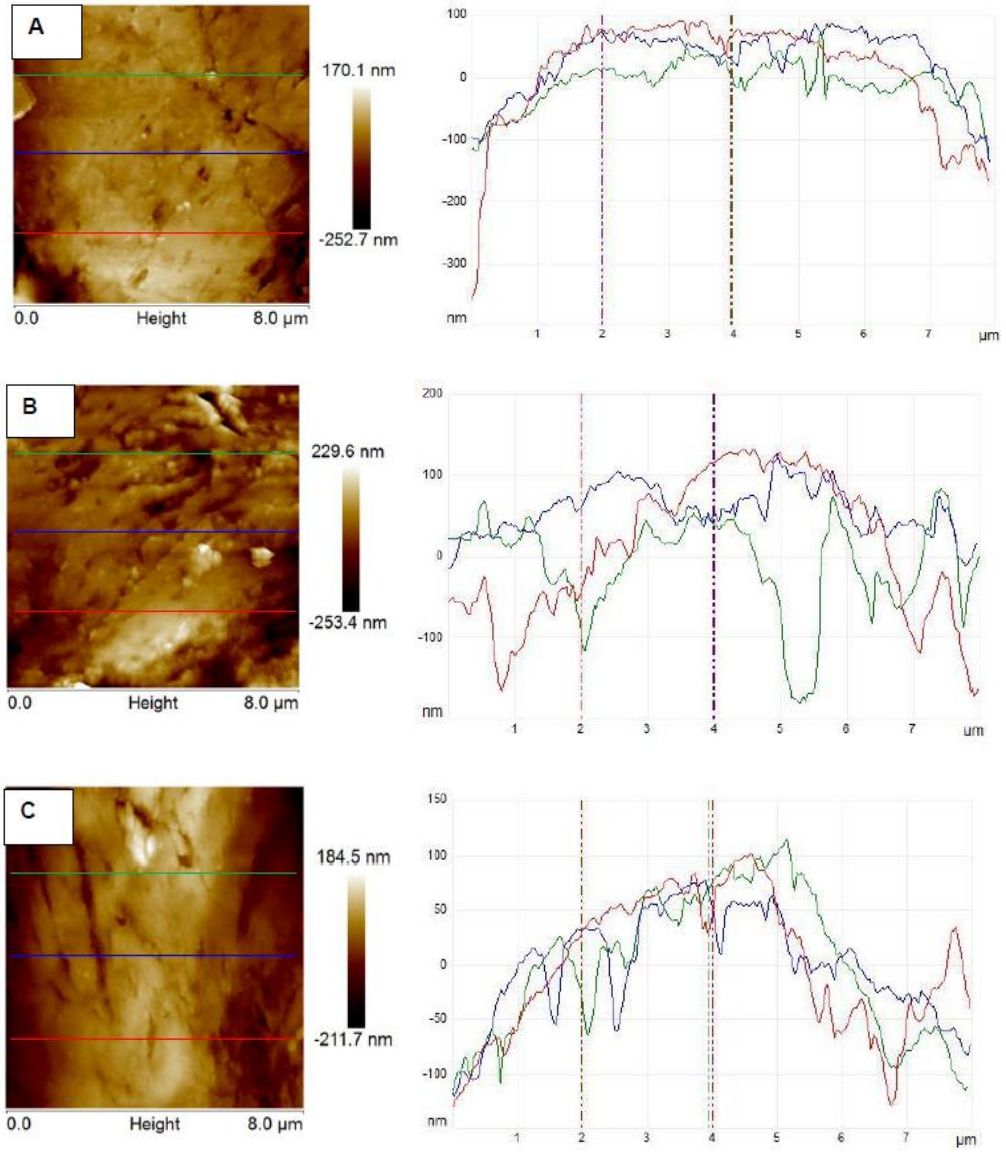

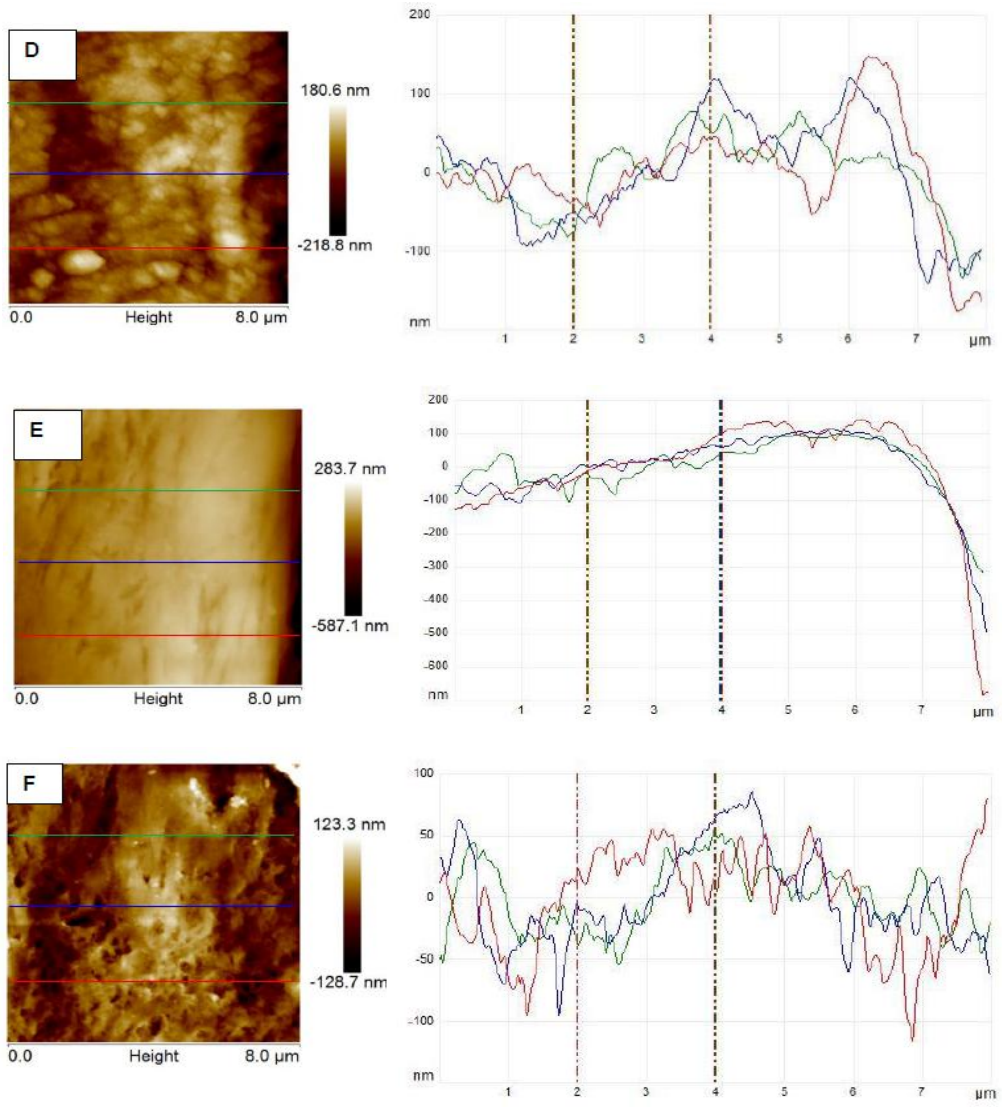


**Fig. 3. Most representative AFM images of topography of human nails**

*Nail pieces were cut from the same healthy human nail clipping before (A, C and E) and after 40 µM porphyrin MFPS treatment (B compared to A), 40% PG treatment (D compared C) and 40 µM MFPS / 40% PG treatment (F compared to E). In each piece of nail 6 spots were chosen and each scanned 3-5 times using tapping mode (tip velocity 32 µm/s). Topography images are shown on the left side while on the right sections (profiles) corresponding to the coloured lines in the topography are shown*

### 3.2 Fungal Nail Infection Largely Determines the Nail's Topography

In case of a14-day infection of human nail clippings with the dermatophyte *T. mentagrophytes* at 37°C and 6.4% $CO_2$ the fungal hyphae have been proven to penetrate the nail plate [6]. This fungal penetration starts from initial attachment of inoculated conidia to ventral and dorsal nail plate sides, subsequent germination and further hyphae development [16]. Infection conditions allow *T. mentagrophytes* hyphae to grow inside rather than outside the nail plate. However, the topography of such onychomycosis nails on the nanoscale will be largely determined by fungal hyphen populating nail's surface (Fig. 4A). Selected profiles in the topographical 14-day *ex vivo T. mentagrophytes* onychomycosis image indeed showed a large spreading (compare the height profiles in Fig. 3A to those in Fig. 4A). Notice that our previous scanning electron microscope (SEM) study already illustrated dermatophytic morphology and dimension

characteristics on human skin [17]. In this study we also noticed filamentous structures with widths of approximately 2-3 µm and rough, fibre-like surfaces. Fig. 4A image may therefore match fungal morphology thereby explaining increased profiles. Additionally, image $Rq$ values were calculated and data shown in Table 2. Again in both onychomycosis nail parts large differences were found in the image $Rq$ values between selected spots. For comparison topographical characteristics of *ex vivo* induced onychomycosis was compared with clinical onychomycosis (Fig. 4B). Notice the more smooth topography in case of the clinical fungal nail infection. In *ex vivo* induced onychomycosis the infection starts from the outer nail parts first in contrast to *in vivo* cases where the infecion infiltrates the nailplate interior mostly from nail root and eponychium. This may explain topographical differences between the two onychomycoses [18].

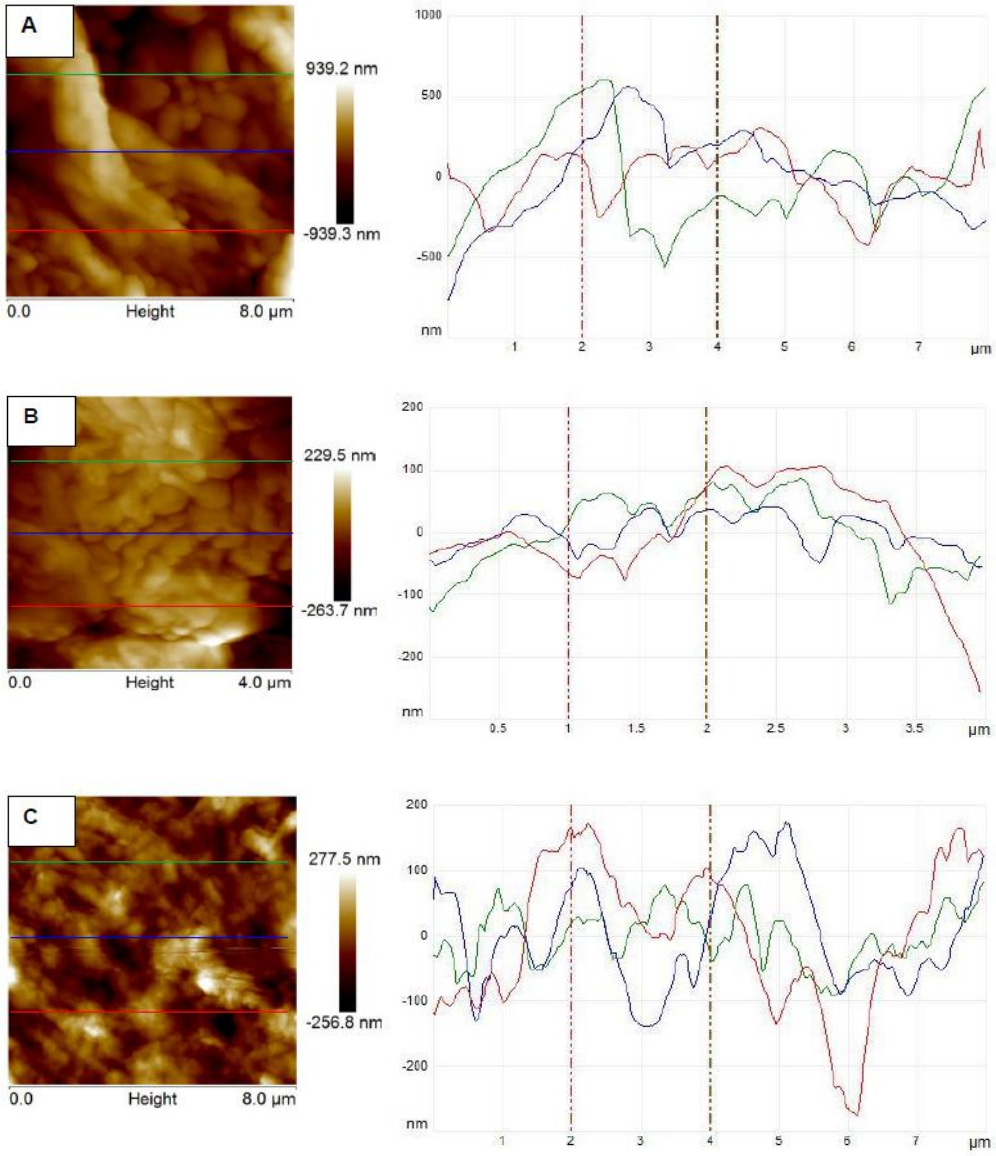


**Fig. 4. Most representative AFM images of topography of *ex vivo* induced 14-day *T. mentagrophytes* onychomycosis (A) Compared to clinical *T. rubrum* onychomycisis (B)**

*C: Representative image of ex vivo induced onychomycosis nails after treatment with 40 µM MFPS in 40% PG. Graphs on the right side represent profiles corresponding to the coloured lines in the topographical image on the left. In each infected nail part 6 spots were chosen and scanned 3-5 times using tapping mode*

**Table 1. Roughness ($R_q$) of 8 x 8 µm scanned spots on nails parts before and after various treatments**

| Nail part[1]: Treatment | $R_q$ ± SD (nm) spot (number of scans) | | | | | | Mean $R_q$ ± SD (nm) |
|---|---|---|---|---|---|---|---|
| | 1 | 2 | 3 | 4 | 5 | 6 | |
| 1: Healthy untreated | 70±4(5) | 87.6±0.5(4) | 84±3(4) | 80±3(6) | 68±1(4) | - | 80±9 |
| 1a: MFPS treated[2] | 45±4(3) | 56±3(5) | 72±6(4) | 74±5(7) | 69±2(5) | - | 66±12 |
| 2: Healthy untreated | 148±7(3) | 99±9(6) | 56±4(4) | 196±2(5) | 80±16(7) | - | 113±48 |
| 2a: MFPS[3] treated | 146±9(8) | 117±1(3) | 99±21(3) | 155±12(7) | 72±10(10) | - | 117±35 |
| 3: Healthy untreated | 310±10(3) | 77±6(7) | 111±3(4) | 340±1(3) | 52±1(5) | 107±2(6) | 137±104 |
| 3a: PG[4] treated | 363±38(4) | 74±4(5) | 143±11(4) | 373±9(4) | 59±8(4) | 79±4(6) | 207±184 |
| 4: Healthy untreated | 132.3±0.5(6) | 218±5(4) | 157±12(10) | 262±21(5) | 133±12(5) | - | 174±50 |
| 4a: PG treated | 120±0.8(4) | 176±17(9) | 134±4(6) | 305±4(4) | 80±1(5) | - | 160±67 |
| 5: Healthy untreated | 240±16(5) | 273±21(6) | 218±10(3) | 153±12(4) | 140±8(4) | 183±5(5) | 188±70 |
| 5a: MFPS/PG treated | 227±11(10) | 277±11(7) | 108.7±0.6 (3) | 90±2(4) | 74.7±0.4(3) | 74.1±0.2(3) | 184±80 |
| 6: Healthy untreated | 121±14(3) | 143±13(5) | 110±1(4) | 144±3(4) | 134±12(4) | 172±14(4) | 138±22 |
| 6a: MFPS/PG treated | 58±2(7) | 161±4(3) | 90±2(5) | 65±3(4) | 82±2(5) | 175±2(3) | 84±41 |

*[1]All nail parts were obtained from the same nail clipping, [2]All treatments lasted 40 hours, [3]MFPS concentrations: 40 µM, [4]PG concentration: 40% (v/v)*

**Table 2. Roughness ($R_q$) of 8 x 8 µm scanned spots on onychomycosis nail parts before and after treatment with MFPS/PG formulation**

| Nail part[1]: Treatment | $R_q$ ± SD (nm) spot (number of scans) | | | | | | Mean $R_q$ ± SD (nm) |
|---|---|---|---|---|---|---|---|
| | 1 | 2 | 3 | 4 | 5 | 6 | |
| 1: Onychomycosis nail | 275±53(5) | 455±86(5) | 680±74(4) | 298±12(5) | 279±6(5) | 361±8(3) | 368±140 |
| 1a: MFPS/PG treated[2] | 145±20(4) | 262±2(4) | 297±20(4) | 150±2(4) | 89±27(3) | 150±22(4) | 164±71 |
| 2: Onychomycosis nail | 427±6(4) | 274±1(4) | 199±1(4) | 224±3(3) | 195±3(3) | 170±1(5) | 240±88 |
| 2a: MFPS/PG treated[2] | 239±2(4) | 171±2(4) | 111±12(3) | 142±2(3) | 165±5(4) | 123±0(3) | 164±40 |

*[1]Nail parts 1 and 2 were obtained from infected (14 days with T. mentagrophytes) nail clippings; [2]All treatments lasted 40 hours; [3]MFPS concentrations: 40 µM; [4]PG concentration: 40% (v/v)*

### 3.3 MFPS / PG Formulation Changed Onychomycosis Nail's Topography Reducing Height Profiles

As the height profiles of our *ex vivo* induced onychomycoses (Fig. 4A) showed large outliers treatment with the MFPS/PG PDT formulation resulted in more even profiles with loss of characteristic hyphal structures (Fig. 4C compared to Fig. 4A). This flattening of fungal filaments resulting from applied antifungal PDT formulations was also noticed in previous SEM research [17]. Results of the post-treatment image roughness calculations are also given in Table 2. Again a-numbered nail parts cannot be fully compared to corresponding similar numbers because of slight differences in spot selections. Notice furthermore that spreading in $Rq$ measured within a single spot is in most cases also much larger than found in the case of healthy nails (Table 1). However, it may nevertheless be noticed that mean $Rq$ values for infected nail parts after treatment with the MFPS/PG PDT formulation decreased in both cases. This is consistent with the changes in topographical height lines observed in Fig. 4. For comparison, the mean calculated $Rq$ value of the clinical onychomycosis nail part was 33±11 nm, significantly lower than found for the *ex vivo* induced infections. Topographical differences between the *ex vivo* induced compared to clinical nail infection may be caused by differences in infection duration. The topography of a 35-day *ex vivo* induced onychomycosis resembled more the topography as found for the clinical onychomycosis nails (unpublished data). However, our choice for a 14-day *ex vivo* onychomycosis stage was based on the wish to have an appropriate amount nail compared to fungus. Moreover, in a clinical situation nail material wil be constantly renewed while in our *ex vivo* situation emerging fungal growth will eventually deplete nail's keratin.

### 3.4 MFPS and PG Decreased Human Nail's Young's Modulus

Direct proof for human nail penetration enhancement effectiveness of our MFPS, one of the functions of this newly designed molecule, was obtained through indentation measurements. AFM indentation is performed by acquiring F-D curves while the same probe used for imaging moves from not touching the sample surface (large separations), to touching the surface (intermediate separations), to strongly touching the surface and pushing/indenting the surface (small separations). The deflection of the elastic cantilever is measured. By choosing a cantilever that is stiffer than the sample, the deflection is a measure of the deformation of the sample. Typical F-D curves of human healthy and *ex vivo* onychomycosis nails are given in respectively Figs. 5A and 5B.

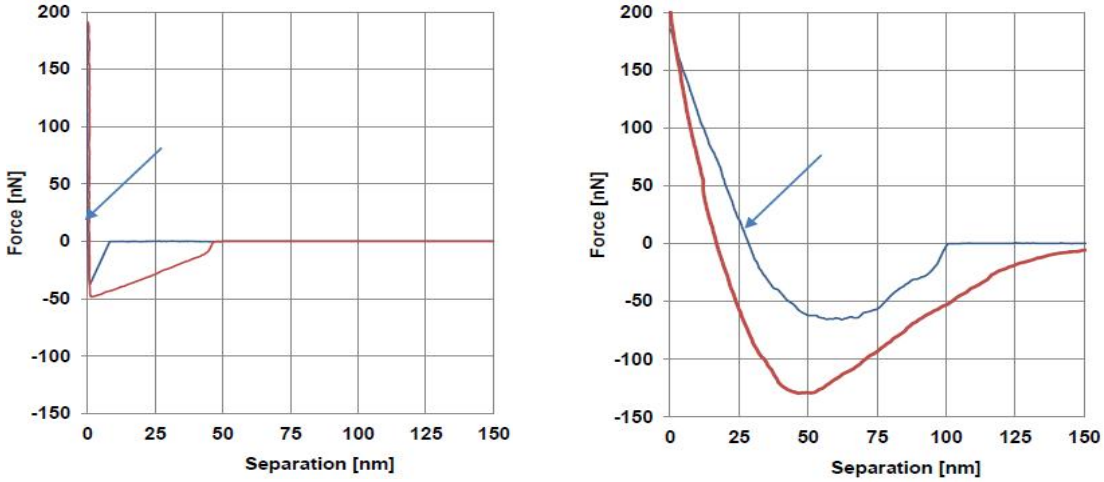


**Fig. 5. Typical indentation curves of a human healthy nail sample (A) and an *ex vivo* induced onychomycosis nail sample**

*The blue lines indicate approach curves (AFM probe moving towards the surface) while red lines correspond to retraction curves (AFM probe moving away from the surface). The separation (nm) given on the axis is defined as the distance between tip and maximum indentation point. Both arrows point to the blue curve parts that were used for fitting in the Hertz model to obtain Young's modulus.*
*Poisson ratio: 0.3; tip radius: 8 nm; tip half angle: 18°*

When comparing the curves from Fig. 5A to those given in part Fig. 5B it can be seen that the blue retraction curve from A is much steeper than corresponding curve in B. This observation and the larger separation values already indicate higher strength for the healthy nail sample (curves in Fig. 5A) compared to the onychomycosis nail sample (curves in Fig. 5B). Moreover, even a stronger (higher) spring constant for the onychomycosis measurements (Fig. 5B still resulted in a weaker response. Based on all indentation data we calculated the Young's modulus (Table 3) of nail parts before and after various chemical treatments using the Herzt model.

Part A of Table 3 gives the values for healthy nail parts before and after treatment with PG (40%), MFPS (40 µM) and a combination of both while part B shows these values obtained for *ex vivo* induced onychomycoses before and after treatment with 40 µM in 40% PG. Noticeable are the large differences between Young's moduli for the two different nail parts cut from the same nail clipping. Values varied from 1 to 27 GPa for healthy parts (Table 3A). This underlines the inhomogeneous character of human nail plates. This difference in hardness of the human nail keratin may be responsible for the large variation always reported in responses to currently available antifungals [19]. Apart from the fact that common antifungals hardly affect fungal spores this variation in hardness in the nail plate may therefore also account for localised differences in response to antifungal drugs (stiff and less stiff nail plate areas alternate leading to alternating drug susceptibility). It may be worthwhile to mention that our healthy nail Young's modulus values were higher than reported corresponding values for horse hoofs (0.4 GPa, determined by tensile measurements) [20], the keratin material that is often applied in nail penetration studies as human nail substitute. Compared to other literature our range of mechanical human nail keratin strength is also larger than reported for different human trichocyte keratins. Chou and Buehler for example mentioned for different trichocyte keratins an elastic modulus ranging from 1 to 4 GPa [7]. Young's modulus values depend also on the method that is used for their determination. This is well explained by Mckee et al. [21]. This group demonstrated for soft biological tissues differences in Young's modulus values when obtained with indentation compared to tensile measurements. Tensile studies usually resulted in larger values. In a study of Seshadri and Bhushan mechanical properties of human hair were studied with AFM stress-strain curves and elastic modulus values varied from 1 to 3.5 GPa [22]. However, human hair AFM indentation measurements resulted in Young's moduli that ranged from 5 to 78 GPa [23].

Despite our large variation in Young's modulus observed for healthy nail parts all PG and MFPS treated parts showed a significant ($p$ < 0,0001) reduction of this mechanical property (Table 3-A). Reduction of the Young's modulus was in both our tests 70% for PG and 85% for our MFPS. This weakening effect is consistent with the specific nail penetration effect of PG that is known to disrupt weak H-bonding (representing 5-30 kJ/mol) while our MFPS chemically cuts S-S covalent bindings (representing approximately 250 kJ/mol). The nail penetration effectiveness of a compound that interferes with the disulphide bridges in the nail's keratin may thus in theory achieve a higher nail plate weakening effect. However, to our surprise, treatment of nails under similar conditions with a combined formulation of PG and MFPS did not result in significant changes in Young's modulus. But our study was not the only one reporting similar or increased mechanical strength of biological material upon indentation. Fortier *et al* for instance noticed this phenomenon of increased strength in keratin fibres from human hairs. They explained this observed hardening as being a result from unfolding and refolding of α-helical keratin structure. In our case chemical treatments mainly cause changes in and weakening of the keratin structure that is normally responsible for the nail's strength. The reason for finding similar mechanical strength in our experiments only in case of application of both PG and MFPS may be that this combination has an increased disrupting effect of the keratin structure thereby facilitating hardening upon continuing indentations; the softer the material the more easy it will be pressed. This phenomenon was more distinct noticed for the much weaker onychomycosis nails (Table 3B) where presence of fungal elements on and in the nail appeared to significantly increase the apparent strength of the treated nails. Notice that the increased weakness of human nails after fungal infection may be taken into account in case of drug penetration studies that always employ strong intact nail plates. For this and other reasons like drug-fungus interactions (unpublished onychomycosis nail penetration results of chemical enhancers) nail permeation studies should include these infected nails as well. In our study 14-day *T. mentagrophytes* nail

**Table 3. Young's modulus calculations of healthy (A) and onychomycosis (B) human nails before and after various treatments based on indentation data and the Hertz model using a Poisson ratio of 0.3**

**(A)**

| Nail condition (nail part) | Young's modulus[1] (GPa ± sd) | Spring constant (N/m) | $P^2$ |
|---|---|---|---|
| Healthy nail (1) | 17±10 | 5.3 | < 0.0001 |
| Healthy nail (1) after PG treatment[3] | 5±3 | 5.5 | |
| Healthy nail (2) | 1.2±0.4 | 3.1 | < 0.0001 |
| Healthy nail (2) after PG treatment | 0.391±0.045 | 2.3 | |
| Healthy nail (3) | 5±3 | 5.5 | < 0.0001 |
| Healthy nail (3) after MFPS treatment | 0.7±0.3 | 4.6 | |
| Healthy nail (4) | 3.2±0.7 | 4.5 | < 0.0001 |
| Healthy nail (4) after MFPS treatment | 0.5±0.3 | 5.0 | |
| Healthy nail (5) | 9±7 | 5 | 0.393 |
| Healthy nail (5) after PG/MFPS treatment | 7±3 | 5.3 | |
| Healthy nail (6) | 18±9 | 5.6 | 0.089 |
| Healthy nail (6) after PG/MFPS treatment | 15±8 | 5.8 | |

**(B)**

| | | | |
|---|---|---|---|
| Onychomycosis[4] nail (1) | 1.2±0.6 | 6.3 | < 0.0001 |
| Onychomycosis nail (1) after PG/MFPS treatment | 4±2 | 5.8 | |
| Onychomycosis nail (2) | 0.14±0.09 | 6.1 | < 0.0001 |
| Onychomycosis nail (2) after PG/MFPS treatment | 5±2 | 5.6 | |

*[1]Indentations were performed on 5 to 6 spots within a selected area of a human nail part before and after treatment. Two different nail parts obtained from the same nail clipping were tested*

*[2]Significance was evaluated using Wilcoxon Signed Ranks test in SPSS statistics 21 with significance evaluated for p = 0.05*

*[3]All treatments lasted 40 h*

*[4]Onychomycosis was induced ex vivo on two different nail parts from the same finger and donor nail and infected with T. mentagrophytes for 14 days (37°C, 6.4 % $CO_2$)*

infections mostly reduced the Young's modulus values significantly ($p$ < 0,0001) with more than 100% to values between 0.05 to 1.8 GPa. Increasing indentation after treatment with our MFPS/PG formulation then caused the Young's modulus to increase again ($p$ < 0.0001) as discussed to apparent values up to 2 to 6 GPa.

## 4. CONCLUSION

This study investigated the effect of a known (PG) and novel (MFPS) chemical nail penetration enhancers on the mechanical strength of healthy and infected human nail plates before and after treatment with these chemicals. In general our study revealed that AFM results are extremely influenced by environmental sample conditions like temperature, sample storage and spot selections. Working as reproducible as possible in every tiny detail is highly recommended for AFM studies like described in this manuscript. An extreme inhomogeneous character within a single human nail plate was found both in terms of roughness and mechanical strength. It may therefore be difficult to develop an antifungal agent that is able to cope with the extremes in nail plate strength and topography. Local differences in nail's strength will influence treatment time and effectiveness. Moreover, the presence of fungus in the nail also influences the mechanical nail strength and may thus alter drug penetration characteristics and efficacy. Finally, as the young's modulus of horse hoofs and human nails differ largely, horse hoofs may not be such a good substitute for antifungal nail penetration testing. Finally the limitations of our

study e.g. choice for only one nail donor and lack of continuous production of keratin in case of our *ex vivo* induced onychomycosis nails should be noticed. In case of clinical onychomycosis nail's keratin will not be gradually consumed but constantly renewed. This may again strengthen these nails. However, the outcome of this study provides physical prove for the reality in clinical practice namely that current treatments may not always be successful. The inhomogeneous nail plate character is probably responsible for the variety in drug responses. With respect to this subject it may be worth to alternate commonly applied antifungals with 40% PG treatment.

## COMPETING INTERESTS

Authors have declared that no competing interests exist.

## REFERENCES


1. Grover C, Khurana A. Onychomycosis: newer insights in pathogenesis and diagnosis. Indian J Dermatol Venereol Leprol. 2012;78:263-70.
2. Cathcart S, Cantrell W, Elewski B. Onychomycosis and diabetes. J Eur Acad Dermatol Venereol. 2009;23:1119-22.
3. Thomas J, Jacobson GA, Narkowicz CK, et al. Toenail onychomycosis: An important global disease burden. J Clin Pharm Ther. 2010;35:497-519.
4. Lehn C, Mutzel E, Rossmann A. Multi-element stable isotope analysis of H, C, N and S in hair and nails of contemporary human remains. Int J Legal Med. 2011; 125:695-706.
5. Smijs T, Dame Z, de Haas ER, et al. Photodynamic and nail penetration enhancing effects of novel multifunctional photosensitizers designed for the treatment of onychomycosis. Photochem Photobiol. 2013;90:189-200.
6. Den Hollander CWJ, Visser J, de Haas ERM, et al. Effective single photodynamic treatment of *ex vivo* onychomycosis using a multifunctional photosensitizer and green light. JoF. 2015;1:138-53.
7. Chou CC, Buehler MJ. Structure and mechanical properties of human trichocyte keratin intermediate filament protein. Biomacromolecules. 2012;13:3522-32.
8. Franck A, Cocquyt G, Simoens P, et al. Biomedical properties of bovine hoof claw horn. Biosys Eng. 2006;93:459-67.
9. Zurita J, Hay RJ. Adherence of dermatophyte microconidia and arthroconidia to human keratinocytes *in vitro*. J Invest Dermatol. 1987;89:529-34.
10. Smijs TG, Bouwstra JA, Schuitmaker HJ, et al. A novel *ex vivo* skin model to study the susceptibility of the dermatophyte Trichophyton rubrum to photodynamic treatment in different growth phases. J Antimicrob Chemother. 2007;59:433-40.
11. Hertz H. Uber die berühring fester elastischer köper. J Reine Angew Mathematik. 188;92:156-71.
12. Johnson KL. Contact Mechanics. 9th ed. Cambridge University Press, New York, US; 2003.
13. Hasnine M, Muhannad M, Suhling JC, Prorok BC, Bozack MJ, Lall P. Nanomechanical characterisation of lead free solder joints. In: Shaw III G, Starman L, Furlong C, editors. MEMS and Nanotechnology, USA: Springer. 2014;5: 16-22.
14. Vaka SR, Murthy SN, O'Haver JH, et al. A platform for predicting and enhancing model drug delivery across the human nail plate. Drug Dev Ind Pharm. 2011;37:72-9.
15. Palliyil B, Lebo DB, Patel PR. A preformulation strategy for the selection of penetration enhancers for a transungual formulation. AAPS Pharm Sci Tech. 2013; 14:682-91.
16. Nenoff P, Kruger C, Ginter-Hanselmayer G, et al. Mycology - an update. Part 1: Dermatomycoses: Causative agents, epidemiology and pathogenesis. J Dtsch Dermatol Ges. 2014;12:188-209.
17. Smijs TG, Mulder AA, Pavel S, et al. Morphological changes of the dermatophyte *Trichophyton rubrum* after photodynamic treatment: A scanning electron microscopy study. Med Mycol. 2008;46:315-25.
18. Goettmann-Bonvallot S. Clinical types of onychomycosis. Ann Dermatol Venereol. 2003;130:1237-43.
19. Baran R, Kaoukhov A. Topical antifungal drugs for the treatment of onychomycosis: an overview of current strategies for monotherapy and combination therapy. J Eur Acad Dermatol Venereol. 2005;19: 21-9.
20. Bertram JE, Gosline JM. Functional design of horse hoof keratin: The modulation of mechanical properties through hydration effects. J Exp Biol. 1987;130:121-36.

21. McKee CT, Last JA, Russell P, et al. Indentation versus tensile measurements of Young's modulus for soft biological tissues. Tissue Eng Part B Rev. 2011;17: 155-64.
22. Seshadri IP, Bhushan B. Effect of rubbing load on nanoscale charging characteristics of human hair characterized by AFM based Kelvin probe. J Colloid Interface Sci. 2008; 325:580-7.
23. Fortier P, Suei S, Kreplak L. Nanoscale strain-hardening of keratin fibres. PLoS One. 2012;7:e41814.

*© 2016 Hosseinzoi et al.; This is an Open Access article distributed under the terms of the Creative Commons Attribution License (http://creativecommons.org/licenses/by/4.0), which permits unrestricted use, distribution, and reproduction in any medium, provided the original work is properly cited.*

*Peer-review history:*
*The peer review history for this paper can be accessed here:*
*http://sciencedomain.org/review-history/12827*